

HRTF Estimation using a Score-based Prior

Etienne Thuillier
Acoustics Lab
Aalto University
Espoo, Finland



Jean-Marie Lemerrier
Signal Processing Group
University of Hamburg
Hamburg, Germany



Eloi Moliner
Acoustics Lab
Aalto University
Espoo, Finland



Timo Gerkmann
Signal Processing Group
University of Hamburg
Hamburg, Germany



Vesa Välimäki
Acoustics Lab
Aalto University
Espoo, Finland



Abstract—We present a head-related transfer function (HRTF) estimation method which relies on a data-driven prior given by a score-based diffusion model. The HRTF is estimated in reverberant environments using natural excitation signals, e.g. human speech. The impulse response of the room is estimated along with the HRTF by optimizing a parametric model of reverberation based on the statistical behaviour of room acoustics. The posterior distribution of HRTF given the reverberant measurement and excitation signal is modelled using the score-based HRTF prior and a log-likelihood approximation. We show that the resulting method outperforms several baselines, including an oracle recommender system that assigns the optimal HRTF in our training set based on the smallest distance to the true HRTF at the given direction of arrival. In particular, we show that the diffusion prior can account for the large variability of high-frequency content in HRTFs.

Index Terms—3D audio, diffusion models, head-related transfer function, spatial audio.

I. INTRODUCTION

Standard head-related transfer function (HRTF) measurements follow a system identification approach whereby a synthetic probe signal is rendered through a loudspeaker, picked-up by microphones located at the entrances of the subject’s ear canals, and used to deconvolve the resulting binaural recording [1]. Repeating the measurement to capture a full HRTF is laborious and time-consuming. The procedure also requires a dedicated anechoic chamber and specialized, calibrated, audio equipment. Methods using non-specialized equipment in echoic environments have been proposed to democratize access to individualized HRTFs, for example, using a living room’s loudspeaker emitting short bursts of exponential sine sweeps [2] or a hand-held smartphone emitting synthetic probe signals in near field [3]. While scalable to the mass-market and cost-effective, these approaches require the subjects to actively undergo a procedure during which they are subjected to unpleasant-sounding synthetic signals.

This issue could be addressed by relying on isolated sound sources occurring in the subject’s surrounding environment. Recently, Jayaram et al. [4] trained a neural network in a supervised fashion to predict the HRTF’s magnitude spectrum using recordings captured from consumer-grade binaural microphones. This method relies on detection of the sound source’s location and composes a full HRTF by aggregating estimates from various direction of arrivals (DoAs). Such an approach could prove particularly advantageous if shown

adaptable to modern earbud headphones, in which microphones are typically offset from the entrances of the ear canals.

In this work, we also propose to leverage binaural recordings of a source in the subject’s everyday environment. However, we suggest using sounds played back by the user over a paired device with known directivity patterns, for example podcast content over a smart speaker, such that the source is known a-priori along with its DoA. This setup leads us to formulating the task of HRTF estimation from a blind inverse problem perspective, i.e. sampling a valid HRTF that is consistent with the observed binaural reverberant measurement, while also estimating the reverberation in the room. The HRTF sampling procedure uses a data-driven prior provided by a diffusion model trained on binaural time-aligned HRTF filter data. We then fit the room acoustics to a parametric model adapted from [5], [6], which we jointly optimize during the HRTF estimation. This follows a recent line of work that applies diffusion models as priors to solve inverse problems in image and audio domains [6]–[8].

Unlike [4], the proposed approach recovers both magnitude and phase estimates. In contrast to a previous signal processing method under a similar setup [9], the prior ensures consistent scaling between measurements. Furthermore, we demonstrate that our approach outperforms a nearest-neighbour oracle baseline which returns the HRTF from the training set that is closest to the true HRTF at the the detected DoA. In particular, the diffusion prior shows a good expressivity in the higher-frequency regions where the HRTF presents large variations across subjects. The size of the diffusion model is modest, potentially allowing for on-device processing.

II. SCORE-BASED DIFFUSION MODEL OF HRTFS

We present here our data-driven prior for time-aligned HRTF features based on continuous-time diffusion-based generative models, also known as score-based models. Score-based models [10], [11] encompass a class of generative models particularly successful at learning complex data distributions such as e.g. natural images or human speech. Here, we employ score-based models to approximate $p(\mathbf{a}|\gamma)$, that is the distribution of time-aligned HRTFs in the frequency domain, denoted as $\mathbf{a} \in \mathbb{C}^{2 \times F}$, conditioned on the DoA γ .

Score-based models operate as iterative Gaussian denoisers: during training, the target data distribution is transformed into a standard Gaussian distribution following a *forward*

diffusion process, incrementally adding noise. Once training is achieved, new data belonging to the data distribution can be generated through the *reverse diffusion process*, which iteratively removes noise from an initial Gaussian sample until a data sample emerges. In continuous-time score-based models [11], this reverse process can be characterized by the following *probability flow* ordinary differential equation (ODE) [12], adopting the parameterization by Karras et al. [13]:

$$d\mathbf{a}_\tau = -\tau \nabla_{\mathbf{a}_\tau} \log p(\mathbf{a}_\tau | \gamma) d\tau, \quad (1)$$

where τ indexes the reverse process flowing from T_{\max} to 0. The diffusion state \mathbf{a}_τ starts from the initial condition $\mathbf{a}_{T_{\max}} \sim \mathcal{N}(0, \sigma(T_{\max})^2 \mathbf{I})$ and terminates at $\mathbf{a}_0 \sim p_{\text{data}}$. We choose a linear noise variance schedule $\sigma(\tau) = \tau$, which defines the Gaussian marginal densities $p_\tau(\mathbf{a}_\tau | \mathbf{a}_0) = \mathcal{N}(\mathbf{a}_\tau; \mathbf{a}_0, \sigma(\tau)^2 \mathbf{I})$. The *score* $\nabla_{\mathbf{a}_\tau} \log p(\mathbf{a}_\tau | \gamma)$ is intractable at inference for complex distributions. Therefore, a *score model* parameterized with a deep neural network (DNN) $\mathbf{s}_\theta(\mathbf{a}_\tau, \tau, \gamma)$ is trained to estimate the score using *denoising score matching* [14].

III. BINAURAL ROOM IMPULSE RESPONSE PARAMETERIZATION

In a static setup where source and receiver locations are fixed, binaural reverberation can be modelled by convolving an anechoic source \mathbf{s} with the impulse response of the system, i.e. the binaural room impulse response (BRIR) \mathbf{h} . The BRIR is composed from the contributions of wavefronts traveling from the source to the ears of the subject following direct and indirect propagation paths. In this work, we model the BRIR as the sum of an anechoic and a reverberant component:

$$\mathbf{h}_{\mathbf{a}}^{(\psi)} := \begin{bmatrix} \delta_{t_{\text{left}}} \\ \delta_{t_{\text{right}}} \end{bmatrix} * \left(g \begin{bmatrix} \delta_0 \\ \delta_{t_{\text{id}}} \end{bmatrix} * \mathcal{F}^{-1}(\mathbf{a}) + \mathbf{r}^{(\chi)} \right), \quad (2)$$

where $\psi = \{t_{\text{left}}, g, t_{\text{id}}\} \cup \chi$ denotes the optimizable parameters of the model, and \mathbf{a} is the binaural time-aligned HRTF [15] at the given DoA. The HRTF is defined in the frequency domain, hence its time-domain equivalent called head-related impulse response is obtained via inverse Fourier transform \mathcal{F}^{-1} . The symbol δ_t denotes a Kronecker delta delayed by t seconds, $t_{\text{left}} \in [0, \infty)$ models time of flight to the subject's left ear, $g \in (0, 1]$ represents a real-valued attenuation constant, $t_{\text{id}} \in \mathbb{R}$ denotes the inter-aural time difference (ITD) taking the left ear as the reference (non-delayed) channel, and $\mathbf{r} \in \mathbb{R}^{2 \times N_r}$ denotes the reverberant component of the model.

The reverberant component \mathbf{r} is implemented as a binaural variant of a previously proposed parametric model fitting the reverberant characteristics of the room [5], [6]:

$$\mathbf{r}^{(\chi)} := \mathcal{F}_{ST}^{-1} \left(\text{interp.} \left([w_b e^{-m\alpha_b}]_{(c,m,b)} \right) \odot [e^{j\phi_{c,m,f}}]_{(c,m,f)} \right), \quad (3)$$

where $\chi = \{[\alpha_b]_b, [w_b]_b, [\phi_{c,m,f}]_{c,m,f}\}$ denotes the learnable parameters of \mathbf{r} , \mathcal{F}_{ST}^{-1} denotes the inverse short-time Fourier transform (STFT), \odot denotes the Hadamard element-wise product, $m \in \{1, \dots, M_r\}$ indexes over STFT frames, $f \in \{1, \dots, F\}$ over Fourier bins, $b \in \{1, \dots, B\}$ over frequency subbands (with $B < F$), and $c \in \{\text{left}, \text{right}\}$.

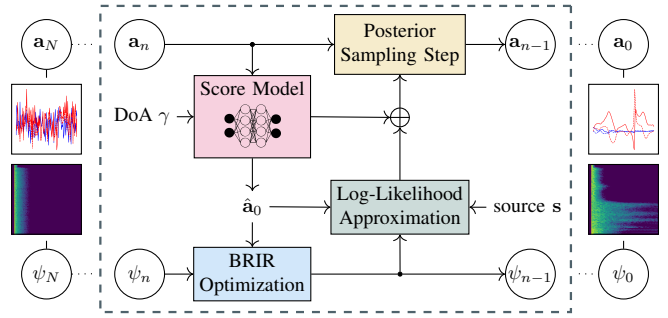


Fig. 1: Diagram of the inference algorithm.

The weight $w_b \in [0, \infty)$ and decay rate $\alpha_b \in [0, \infty)$ define a subband exponential decaying magnitude model, which exploits the observed statistical nature of reverberation tails [16]. Crucially, this magnitude envelope is identical for the left and right channels. The interpolation operator interp. upsamples the B subbands to the F frequency bins of the STFT by employing $\exp(\text{lerp}(\log(\cdot)))$, where lerp denotes linear interpolation. In contrast to the magnitude envelope term, the phase is determined using a specific coefficient $\phi_{c,m,f} \in [\pi, \pi)$ for each channel-frame-bin triplet. This allows for fitting decorrelated left and right channel realizations of the diffuse part, as typically observed in BRIRs above 1 kHz [17], [18]. Additionally, while the early reflections of the BRIR are not explicitly incorporated into the model, the unconstrained phases allow the model to fit these reflections to some extent.

IV. INFERENCE ALGORITHM

The inference process solves the following objective:

$$\hat{\mathbf{a}}, \hat{\psi} = \arg \min_{\mathbf{a}, \psi} \mathcal{C}(\mathbf{y}, \mathbf{h}_{\mathbf{a}}^{(\psi)} * \mathbf{s}) \quad \text{s.t.} \quad \mathbf{a} \sim p_{\text{data}} \quad (4)$$

This means that we wish to retrieve the optimal time-aligned HRTF $\hat{\mathbf{a}}$ and BRIR parameters $\hat{\psi}$ in order to minimize a reconstruction error $\mathcal{C}(\mathbf{y}, \mathbf{h}_{\mathbf{a}}^{(\psi)} * \mathbf{s})$ given and the binaural reverberant measurement \mathbf{y} and the broadband excitation signal \mathbf{s} , which is in our case (but not restricted to) human speech. Another soft constraint is that the estimated time-aligned HRTF $\hat{\mathbf{a}}$ should belong to the target HRTF distribution p_{data} .

We solve (4) using an alternating optimization procedure, visualized in Fig. 1. The acoustic parameters $\hat{\psi}$ in our BRIR model (3) are updated with a classical gradient-based optimizer (e.g. Adam) minimizing the reconstruction loss. The HRTF estimate $\hat{\mathbf{a}}$, however, is refined using a posterior sampling technique leveraging a score model $\mathbf{s}_\theta(\mathbf{a}_\tau, \tau, \gamma)$ trained on time-aligned HRTF data and conditioned on the DoA γ . Precisely, this procedure aims at sampling from the posterior distribution $p(\mathbf{a} | \mathbf{y}, \mathbf{s}, \gamma)$. We leverage our HRTF score-based prior for posterior sampling by solving the ODE (1), where the score function $\nabla_{\mathbf{a}_\tau} \log p(\mathbf{a}_\tau | \gamma)$ is replaced by the so-called *posterior score* obtained via Bayes' formula:

$$\nabla_{\mathbf{a}_\tau} \log p(\mathbf{a}_\tau | \mathbf{y}, \mathbf{s}, \gamma) = \nabla_{\mathbf{a}_\tau} \log p(\mathbf{a}_\tau | \gamma) + \nabla_{\mathbf{a}_\tau} \log p(\mathbf{y} | \mathbf{a}_\tau, \mathbf{s}). \quad (5)$$

The *prior score* $\nabla_{\mathbf{a}_\tau} \log p(\mathbf{a}_\tau | \gamma)$ is obtained via our score model $\mathbf{s}_\theta(\mathbf{a}_\tau, \tau, \gamma)$. Since we generally do not have a model for \mathbf{y} given the diffusion state \mathbf{a}_τ , the likelihood $p(\mathbf{y} | \mathbf{a}_\tau, \mathbf{s})$ is intractable. However, it can be derived using the following approximations, similar to [5]. First, we follow Chung et al. [7] and employ an estimate of \mathbf{a}_0 at time τ as a sufficient statistic for \mathbf{a}_τ in the likelihood. This results in assuming $p(\mathbf{y} | \mathbf{a}_\tau, \mathbf{s}) \approx p(\mathbf{y} | \hat{\mathbf{a}}_0, \mathbf{s})$. The estimate $\hat{\mathbf{a}}_0$ is directly obtained from the unconditional score model via one-step denoising:

$$\hat{\mathbf{a}}_0 := \mathbf{a}_\tau - \sigma(\tau)^2 \mathbf{s}_\theta(\mathbf{a}_\tau, \tau, \gamma). \quad (6)$$

Furthermore, we model binaural reverberation by a convolution between the excitation signal \mathbf{s} and our BRIR model $\mathbf{h}_{\hat{\mathbf{a}}_0}^{(\psi)}$, using the one-step denoising HRTF estimate $\hat{\mathbf{a}}_0$, and assuming $p(\mathbf{y} | \hat{\mathbf{a}}_0, \mathbf{s}) \approx p(\mathbf{y} | \mathbf{h}_{\hat{\mathbf{a}}_0}^{(\psi)} * \mathbf{s})$. Finally, we follow [19] and approximate the log-likelihood gradient using a L^2 -distance in the magnitude-compressed STFT domain, between the measurement and our estimate:

$$\mathcal{C}(\mathbf{y}, \hat{\mathbf{y}}) = \frac{1}{M_{\mathbf{y}}} \|\mathcal{S}_{\text{comp}}(\mathbf{y}) - \mathcal{S}_{\text{comp}}(\hat{\mathbf{y}})\|_2^2, \quad (7)$$

where $\mathcal{S}_{\text{comp}}(\mathbf{y}) := |\mathcal{F}_{\text{ST}}(\mathbf{y})|^{2/3} \exp j \angle \mathcal{F}_{\text{ST}}(\mathbf{y})$ is the magnitude-compressed spectrogram with $M_{\mathbf{y}}$ STFT frames. This compression accounts for the heavy-tailedness of speech distributions [20]. Note that we also use this function as the objective for optimizing the BRIR parameters ψ in (4). The log-likelihood gradient is finally obtained as:

$$\nabla_{\mathbf{a}_\tau} \log p(\mathbf{y} | \mathbf{a}_\tau, \mathbf{s}) \approx -\zeta(\tau) \nabla_{\mathbf{a}_\tau} \mathcal{C}(\mathbf{y}, \mathbf{h}_{\hat{\mathbf{a}}_0}^{(\psi)} * \mathbf{s}), \quad (8)$$

where $\zeta(\tau)$ adjusts the weight of the log-likelihood gradient during sampling, and is parameterized following [5], [8]. In conclusion, the posterior sampling procedure amounts to solving the following ODE:

$$d\mathbf{a}_\tau = -\tau \left[\mathbf{s}_\theta(\mathbf{a}_\tau, \tau, \gamma) - \zeta(\tau) \nabla_{\mathbf{a}_\tau} \mathcal{C}(\mathbf{y}, \mathbf{h}_{\hat{\mathbf{a}}_0}^{(\psi)} * \mathbf{s}) \right] d\tau, \quad (9)$$

In summary, the resulting algorithm alternates between optimizing BRIR parameters and estimating the HRTF, as illustrated in Fig. 1. At each step n of the discretized diffusion time axis, we perform N_{its} optimization iterations of the parameters ψ_n in our BRIR model (3), followed by a sampling step of the ODE (9) to update the HRTF estimate \mathbf{a}_n .

V. EXPERIMENTAL SETUP

A. Experimental Data

HRTF data: We obtain the time-aligned features required to train the score model and evaluate our HRTF estimation method from the simulated HRTF sets of the HUTUBS database [21]. In practice, the pure delay component is estimated and removed from the channel of each HRTF data point. This yields 2×128 -dimensional binaural time-aligned HRTF spectra after dropping the Nyquist bin (more details in [22], [23]). Out of the 95 HUTUBS subjects, 85 are used to train the score model. Two subjects are reserved for validation and six for testing. Repeated simulations “88” and “96” of HUTUBS subjects “1” and “22” are excluded from our splits.

TABLE I: *Instrumental results obtained on simulated 44.1-kHz BRIR data. Values indicate mean and standard deviation. Lower is better*

Method	LRE	LMD
Random	-3.43 ± 1.59	4.58 ± 0.69
Generic	-4.01 ± 1.75	4.77 ± 0.74
Proposed	-9.20 ± 5.64	2.28 ± 1.11
<i>Nearest Neighbour</i>	-7.50 ± 1.46	3.76 ± 0.61

Estimation task data: We evaluate the performance of our HRTF estimation method using reverberant binaural speech observations generated by filtering utterances from VCTK’s speakers “p226” and “p287” [24] with simulated BRIRs. The BRIRs are generated using a publicly available shoebox simulation software implementing the image-source method [25], [26], which we set to a reflection order of 20. We provide the software with our test HRTFs for binauralization of the room impulse response. Approximately 100 tasks were generated per test subject for a total of 599.

In each estimation task, the room’s height is drawn uniformly in the [2.5, 4] m range and the floor dimensions (width and length) in the [7, 15] m range. The source and the subject’s head locations is drawn uniformly within the volume of the room at a distance of at least 1.5 m from the walls and with a height in the [1, 2] m range. The source is maintained at least 1 m away from the subject’s head and its location is slightly adjusted so that it matches the closest DoA from the subject’s HRTF set. Finally, the absorption coefficient of the simulation model is drawn within the [0.05, 0.1] range. A similar validation set was generated for tuning the hyperparameters of our method using the HUTUBS subjects from our validation split. The VCTK recordings were down-sampled to 44.1 kHz prior to filtering so as to match the simulation’s sample rate.

B. Implementation Details

Diffusion Parameterization The score model is trained using diffusion times between $T_{\text{min}} = 0.01$ and $T_{\text{max}} = 10$. At inference time, we reduce the extremal times to $T_{\text{min}} = 0.05$ and $T_{\text{max}} = 8$ as they showed to be sufficient. The above levels are relative to normalized HRTF features, which are obtained by scaling the original features with respect to the mean and variance of our training set. We discretize the diffusion time axis into $N = 100$ steps for reverse diffusion using the logarithmic discretization in [13].

DNN Architecture: We parameterize the HRTF score model with a 1D-UNet comprising seven encoding-decoding stages, each with a resampling factor of 2 and comprising 32 hidden features. The model encodes the DoA γ and the diffusion time τ using random Fourier features embedding [27]. The above architecture results in a total of 752k parameters which we optimize using Adam with a learning rate of 5×10^{-4} and batch size of 32 for 110k steps. During training, we prevent the model from relying too heavily on DoA information by

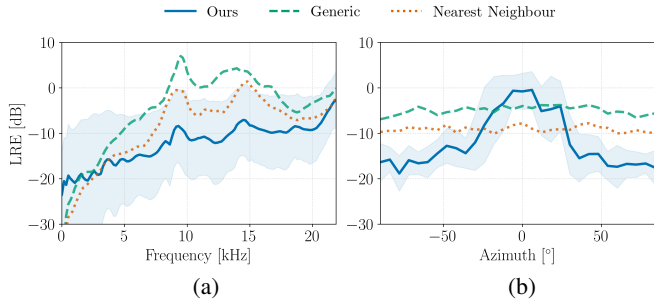


Fig. 2: LRE as a function of (a) frequency and (b) azimuth.

injecting white noise ($\sigma = 0.05$) in the value of γ , and even completely dropping out γ with a probability of 30%. We track an exponential moving average of the DNN weights with a decay of 0.999.

BRIR Model: STFTs are computed using a Hann window of 23 ms and 75% overlap. We set the number of STFT frames of our reverberation operator to $M_r = 200$, which corresponds to 120 ms. We decimate the frequency scale into $B = 40$ bands using a quasi-logarithmic spacing [6]. We optimize the BRIR parameters ψ with Adam [28], with a learning rate of 0.01, momentum parameters of $\beta_1 = 0.9$ and $\beta_2 = 0.999$, and $N_{\text{its}} = 50$ optimization iterations per diffusion step. After each optimization step, we further clamp the weights $[w_b]_b$ between 0 and 40 dB, and the decays $[\alpha_b]_b$ between 0.01 and 40. This helps stabilize the optimization at early sampling stages. The parameters are initialized to $g = 0.15$, $t_{\text{left}} = 52$ samples, $w_b = 2$ and $\alpha_b = 0.1$ (across all frequency bands). Finally, t_{itd} is initialized according to the DoA.

C. Evaluation

We report the performance of our method in terms of logarithmic relative error (LRE)

$$\text{LRE}(\mathbf{a}_{c,f}, \hat{\mathbf{a}}_{c,f}) = 20 \log_{10} \left| \frac{\hat{\mathbf{a}}_{c,f} - \mathbf{a}_{c,f}}{\mathbf{a}_{c,f}} \right|, \quad (10)$$

and log-magnitude distance (LMD)

$$\text{LMD}(\mathbf{a}_{c,f}, \hat{\mathbf{a}}_{c,f}) = \left| 20 \log_{10} \left| \frac{\hat{\mathbf{a}}_{c,f}}{\mathbf{a}_{c,f}} \right| \right|. \quad (11)$$

We define three baselines for HRTF estimation: *Random* returns an HRTF filter drawn randomly from the training set at the specified DoA. *Generic* systematically returns HRTF filters from the HRTF subject forming a centroid of the training set, i.e. which minimizes the pairwise error to all the other HRTF subjects of the set as computed using the mean LRE across DoAs, frequencies and binaural channels. *Nearest Neighbour* is a quasi-oracle baseline: it selects, amongst the training set, the HRTF with matching DoA that yields the lowest mean LRE error to the true HRTF.

VI. RESULTS AND DISCUSSION

The results of the objective metrics are reported in Table I. The proposed method outperforms the compared baselines,

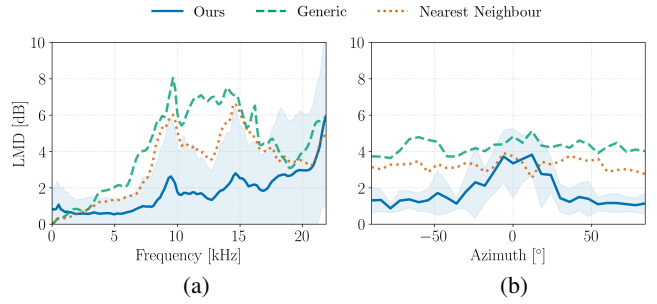


Fig. 3: LMD as a function of (a) frequency and (b) azimuth.

including the *Nearest Neighbour* oracle in both LRE and LMD metrics. Figures 2 and 3 illustrate the instrumental metrics as a function of frequency and azimuth. The results in Figures 2a and 3a reveal several key trends. First, the error increases with frequency, likely due to higher individual variability at higher bands. Notably, in the 5–8 kHz range, our method achieves a mean LRE that is at least 8 dB lower than the *Generic* HRTF baseline. Furthermore, in the higher frequency range (8–17 kHz), the proposed method improves over the *Nearest Neighbour* oracle baseline by at least 6 dB in LRE and 2 dB in LMD. This performance gain highlights that our method surpasses mere data retrieval capabilities, which we attribute to the modeling capacity of the score-based prior. At lower frequencies (0–1 kHz), the error is slightly higher than the *Generic* baseline and *Nearest Neighbour*. However, this occurs below the range in which lie the most salient monaural cues, in particular filtering from the pinna (>3 kHz) [29].

One area of concern is the increased LRE observed in Fig. 2b at the median plane, i.e. 0° azimuth. In terms of LMD, the proposed solution also suffers from lower performance at the median plane, but our method still outperforms the *Generic* HRTF and is on par with the *Nearest Neighbour* baseline in this worst azimuth case. This suggests that the phase estimation (only assessed in the LRE metric) seems to suffer more than the magnitude estimation in this region. This overall phenomenon may be due to inherent challenges in modeling HRTFs at this spatial position, but this warrants further investigation.

VII. CONCLUSION

This paper proposed a posterior sampling scheme for HRTF estimation using a diffusion-based prior and a parametric reverberation model for approximating log-likelihood computation. Compared to previous approaches, the proposed method can use natural-sounding sources such as speech, requires only one measurement, and more importantly, it can operate in a variety of reverberant environments. At the exception of target directions in the median plane, our method largely outperforms the considered baselines, including an oracle recommender system. In relative terms, the time-aligned HRTF estimation error is particularly low in the high-frequency region, which we attribute to the expressivity of the diffusion prior.

REFERENCES

- [1] V. R. Algazi, R. O. Duda, D. M. Thompson, and C. Avendano, "The CIPIC HRTF database," in *Proceedings of the IEEE Workshop on the Applications of Signal Processing to Audio and Acoustics*, 2001, pp. 99–102.
- [2] J. Reijnders, B. Partoens, J. Steckel, and H. Peremans, "HRTF measurement by means of unsupervised head movements with respect to a single fixed speaker," *IEEE Access*, vol. 8, pp. 92 287–92 300, 2020.
- [3] Z. Yang and R. R. Choudhury, "Personalizing head related transfer functions for earables," in *Proceedings of the ACM SIGCOMM Conference*, 2021, pp. 137–150.
- [4] V. Jayaram, I. Kemelmacher-Shlizerman, and S. M. Seitz, "HRTF estimation in the wild," in *Proceedings of the 36th Annual ACM Symposium on User Interface Software and Technology*, 2023, pp. 1–9.
- [5] E. Moliner, J.-M. Lemerrier, S. Welker, T. Gerkmann, and V. Välimäki, "BUDDY: Single-channel blind unsupervised dereverberation with diffusion models," in *Proc. IWAENC*, 2024.
- [6] J.-M. Lemerrier, E. Moliner, S. Welker, V. Välimäki, and T. Gerkmann, "Unsupervised blind joint dereverberation and room acoustics estimation with diffusion models," *arXiv preprint arXiv:2408.07472*, 2024.
- [7] H. Chung *et al.*, "Diffusion posterior sampling for general noisy inverse problems," in *Proc. ICLR*, 2023.
- [8] E. Moliner, J. Lehtinen, and V. Välimäki, "Solving audio inverse problems with a diffusion model," in *Proc. ICASSP*, 2023.
- [9] K. Diepold, M. Durkovic, and F. Sagstetter, "HRTF measurements with recorded reference signal," in *Proceedings of the Audio Engineering Society 129th Convention*, 2010.
- [10] J. Ho, A. Jain, and P. Abbeel, "Denoising diffusion probabilistic models," in *Proc. NeurIPS*, 2020.
- [11] Y. Song and S. Ermon, "Generative modeling by estimating gradients of the data distribution," in *Proc. NeurIPS*, 2019.
- [12] B. Øksendal, *Stochastic Differential Equations: An Introduction with Applications*. Journal of the American Statistical Association, 2000, vol. 82.
- [13] T. Karras, M. Aittala, T. Aila, and S. Laine, "Elucidating the design space of diffusion-based generative models," in *Proc. NeurIPS*, 2022.
- [14] P. Vincent, "A connection between score matching and denoising autoencoders," *Neural Computation*, vol. 23, no. 7, pp. 1661–1674, 2011.
- [15] Z. Ben-Hur, D. L. Alon, R. Mehra, and B. Rafaely, "Efficient representation and sparse sampling of head-related transfer functions using phase-correction based on ear alignment," *IEEE/ACM Trans. Audio Speech Lang. Process.*, vol. 27, no. 12, pp. 2249–2262, 2019.
- [16] E. A. P. Habets, *Speech Dereverberation Using Statistical Reverberation Models*. London: Springer, 2010, pp. 57–93.
- [17] F. Menzer and C. Faller, "Investigations on modeling BRIR tails with filtered and coherence-matched noise," in *Proceedings of the 127th AES Convention*, 2009, p. 7852.
- [18] J. Fagerström, N. Meyer-Kahlen, S. J. Schlecht, and V. Välimäki, "Binaural dark-velvet-noise reverberator," in *Proceedings of the International Conference on Digital Audio Effects*, 2024, pp. 246–253.
- [19] E. Moliner, F. Elvander, and V. Välimäki, "Blind audio bandwidth extension: A diffusion-based zero-shot approach," *arXiv*, 2024.
- [20] T. Gerkmann and R. Martin, "Empirical distributions of DFT-domain speech coefficients based on estimated speech variances," *Proc. IWAENC*, 2010.
- [21] F. Brinkmann, M. Dinakaran, R. Pelzer, P. Grosche, D. Voss, and S. Weinzierl, "A cross-evaluated database of measured and simulated HRTFs including 3D head meshes, anthropometric features, and headphone impulse responses," *J. Audio Eng. Soc.*, vol. 67, no. 9, pp. 705–718, Sep. 2019.
- [22] J. Nam, J. S. Abel, and J. O. Smith III, "A method for estimating interaural time difference for binaural synthesis," in *Proc. Audio Eng. Soc. Conv. 125*, Oct. 2008.
- [23] E. Thuillier, C. T. Jin, and V. Välimäki, "HRTF interpolation using a spherical neural process meta-learner," *IEEE/ACM Transactions on Audio, Speech, and Language Processing*, vol. 32, pp. 1790–1802, 2024.
- [24] C. Valentini-Botinhao *et al.*, "Reverberant speech database for training speech dereverberation algorithms and TTS models," *University of Edinburgh*, 2016.
- [25] R. Barumerli, D. Bianchi, M. Geronazzo, and F. Avanzini, "SofaMyroom: a fast and multiplatform "shoebox" room simulator for binaural room impulse response dataset generation," *arXiv preprint arXiv:2106.12992*, 2021.
- [26] S. M. Schimmel, M. F. Muller, and N. Dillier, "A fast and accurate "shoebox" room acoustics simulator," in *Proc. IEEE International Conference on Acoustics, Speech and Signal Processing*, 2009, pp. 241–244.
- [27] M. Tancik, P. Srinivasan, B. Mildenhall, S. Fridovich-Keil, N. Raghavan, U. Singhal, R. Ramamoorthi, J. Barron, and R. Ng, "Fourier features let networks learn high frequency functions in low dimensional domains," in *Proc. NeurIPS*, 2020.
- [28] D. P. Kingma and J. Ba, "Adam: A method for stochastic optimization," *Proc. ICLR*, 2015.
- [29] C. Jin, A. Corderoy, S. Carlile, and A. van Schaik, "Contrasting monaural and interaural spectral cues for human sound localization," *J. Acoust. Soc. Am.*, vol. 115, no. 6, pp. 3124–3141, 2004.